Strong interference effects in the $e^- + Sc^{3+}$ recombination cross section

T. W. Gorczyca
Department of Physics, Western Michigan University, Kalamazoo, Michigan 49008

M. S. Pindzola and F. Robicheaux
Department of Physics, Auburn University, Auburn, Alabama 36849

N. R. Badnell
Department of Physics and Applied Physics, University of Strathclyde, Glasgow G4 0NG, United Kingdom

(Received 8 July 1997)

The $e^- + Sc^{3+}$ recombination cross section exhibits a strong interference between the radiative and dielectronic recombination pathways at low energies. The resonances associated with the $3p^5 3d^2\,{}^2F$ term in Sc^{2+} are found to have unusually large autoionization widths. Their strong interference with the background radiative recombination results in quite distinct asymmetric resonance profiles. Current ion storage ring experiments should be able to verify the strength of the interference effects.
[S1050-2947(97)06612-2]

PACS number(s): 34.80.Lx

I. INTRODUCTION

Electron recombination with an atomic ion follows two dominant pathways. Radiative recombination (RR) involves the direct transition of a continuum electron to a bound state of the recombined ion with the emission of a photon. Dielectronic recombination (DR) is an indirect process involving the capture of the continuum electron to a doubly excited resonant state of the recombined ion followed by a stabilizing radiative transition. Since the initial and final states of both processes may be the same, quantum mechanical interference between the two pathways can take place. Over the years a number of theoretical approaches have been developed which unify the two recombination processes. The most popular have been a time-dependent approach [1–5] and a general projection operator approach [6–8]. Most recently, *R*-matrix methods based on quantum defect theory [9,10] and a radiative optical potential [11,12] have provided unified computational approaches that can be easily applied to any atomic ion.

Although an example of RR-DR interference has been observed [13] in an ion trap experiment, there still exists no clear example of RR-DR interference in the current generation of ion storage ring experiments [14]. In general [15], the strong resonances are predicted to have interference effects of less than 1%, while only certain weak resonances may exhibit strong interference effects. In the ion storage ring experiments, which measure the total recombination cross section, the weak resonances are buried under their more dominant brethren. On the other hand, the ion trap experiments measure partial recombination cross sections resolved as the final state of the recombined ion. This increases the chances that interference effects in weak resonances can be observed [16]. The main drawback with the ion trap experiments is that the recombination cross section is measured for a mixture of different atomic ions.

Of course, the fact that RR-DR interference effects are generally small is good news for astrophysical and laboratory plasma research, since most of their atomic data in the form of recombination rate coefficients is based on independent calculations for radiative and dielectronic recombination. However, it would be useful to have an ion storage ring experimental benchmark for the recent unified computational methods. In this paper we report on the finding of unusually large RR-DR interference effects in the total recombination cross section for Sc^{3+} at low energies. Both unified distorted-wave and close-coupling calculations predict that the unusual resonance structures are associated with the $3p^5 3d^2\,{}^2F$ terms in the recombined Sc^{2+} ion. They should be easily observed in an ion storage ring experiment. In Sec. II we outline the theory of RR-DR interference, in Sec. III we present our recombination cross section results for Sc^{3+}, and in Sec. IV we conclude with a brief summary.

II. THEORY

A. Distorted-wave method

With the aid of the principle of detailed balance, the total photorecombination (PR) cross section from a continuum state j to a bound state i is given by (in atomic units)

$$\sigma_{\mathrm{PR}}(j \to i) = \frac{g_i}{g_j} \frac{\omega^2}{c^2 k^2} \sigma_{\mathrm{PI}}(i \to j), \tag{1}$$

where $\sigma_{\mathrm{PI}}(i \to j)$ is the photoionization (PI) cross section from a bound state i to a continuum state j, including radiation damping. In Eq. (1), ω is the frequency of the radiation field, c is the speed of light, k is the free electron linear momentum, g_i is the statistical weight of the final recombined ion, g_j is the statistical weight of the initial target ion.

From bound-continuum configuration-interaction theory [17] or diagrammatic many-body perturbation theory [18],

the photoionization cross section, including interference between the resonances and the background in lowest order, may be written as

$$\sigma_{\rm PI}(i\to j)=\frac{8\pi\omega}{3ck}\left|\langle\psi_j|\mathbf{r}|\psi_i\rangle\left(1-i\sum_n\frac{\frac{1}{2}A_a(n\to j)}{\Delta_n+i\frac{1}{2}\Gamma_n\eta_n}\right)+\sum_n\frac{\langle\psi_j|r_{12}^{-1}|\psi_n\rangle\langle\psi_n|\mathbf{r}|\psi_i\rangle}{\Delta_n+i\frac{1}{2}\Gamma_n\eta_n}\right|^2, \tag{2}$$

where $|\psi_i\rangle$ is a bound state, $|\psi_n\rangle$ is a resonance state, $|\psi_j\rangle$ is a continuum state, Δ_n is the energy detuning from resonance, and the continuum normalization is one times a sine function. The autoionization and radiative rates are given by

$$A_a(n\to j)=\frac{4}{k}|\langle\psi_j|r_{12}^{-1}|\psi_n\rangle|^2 \tag{3}$$

and

$$A_r(n\to i)=\frac{4\omega^3}{3c^3}|\langle\psi_i|\mathbf{r}|\psi_n\rangle|^2, \tag{4}$$

while $\Gamma_n=\Sigma_{j'}A_a(n\to j')$, $\gamma_n=\Sigma_{i'}A_r(n\to i')$, and $\eta_n=1+\gamma_n/\Gamma_n$. The resonance energies, bound and continuum wave functions, matrix elements, and rates needed to evaluate Eqs. (1)–(4) for the total recombination cross section for any atomic ion are calculated using the AUTOSTRUCTURE package [19,20].

B. *R*-matrix method

Interference between radiative and dielectronic recombination may be taken into account in a nonperturbative manner through the application of the *R*-matrix method. In order to treat photorecombination within the *R*-matrix formalism, we use the radiative optical potential method [11] to incorporate a one-photon operator into the close-coupling Hamiltonian. The robust Belfast *R*-matrix codes [21], with the inclusion of radiative interactions [22], were extensively modified to incorporate this optical potential, as detailed in previous work [11,12,23]. Nevertheless, a brief review of this method follows.

The principle radiative effects in the present study involve recombination to the $3p^6 3d$ ground state of Sc^{2+}. Since this final state resides completely in the atomic region, or the *R*-matrix ''box,'' radiative decay to it proceeds via the imaginary, energy-dependent, nonlocal radiative optical potential

$$V_{\rm rad}=-i\vec{D}|g\rangle\cdot\langle g|\vec{D}, \tag{5}$$

where $|g\rangle$ is the ground-state wave function and $\vec{D}$ is the dipole operator, which takes the following two forms in the length and velocity gauges:

$$\vec{D}=\sqrt{\frac{2\omega^3}{3c^3}}\vec{r}\quad\text{(length gauge)},$$

$$\vec{D}=\sqrt{\frac{2\omega}{3c^3}}\vec{\nabla}\quad\text{(velocity gauge)}, \tag{6}$$

and the photon energy $\omega=E-E_g$ is the difference between the incident electron energy E and the ground-state energy E_g.

This optical potential contributes an additional term to the *R*-matrix Hamiltonian:

$$H_{\alpha\alpha'}\to H_{\alpha\alpha'}-i\sum_b\frac{2\omega_b^3}{3c^3(2J+1)}\langle\alpha||r||g\rangle\langle g||r||\alpha'\rangle. \tag{7}$$

Since this addition is negative imaginary, flux will be lost and the scattering matrix **S** will be nonunitary. The photorecombination cross section within a partial wave can be computed from this degree of nonunitarity as

$$\sigma_{\rm PR}=\sum_L\frac{\pi}{k^2}\frac{(2L+1)(2S+1)}{2(2L_t+1)(2S_t+1)}\times\sum_{i=1}^{n_1}\left(1-\sum_{j=1}^{n_t}\mathbf{S}(L)_{ij}^*\mathbf{S}(L)_{ij}\right), \tag{8}$$

where L and S are the total orbital and spin angular momentum, L_t and S_t are the orbital and spin angular momentum of the target state ($3p^6\,{}^1S$ for Sc^{3+}), n_t is the total number of open channels, n_1 is the number of channels coupled to the target state, and $\mathbf{S}(L)$ is the scattering or S matrix of the partial wave, L. This modification to the R matrix accounts for both the radiative and dielectronic recombination pathways.

Additional radiative effects in the present study involve recombination into the $3p^6 nl$ excited states of Sc^{2+}. These final decay states exist either partially or completely outside of the *R*-matrix ''box,'' which is only large enough to contain up to $n=3$ orbitals. Thus damping to them is instead treated by adding an imaginary term to the energies of the six $3p^5 3d$ target terms of Sc^{3+}, as originally suggested by Hickman [24]. Details of two different implementations of this procedure, one using multichannel quantum defect theory and the other including the $3p^6 nl$ portion of the wave function in the *R*-matrix box and also modifying the asymptotic energy of the nl valence electron, are detailed in earlier work [11,12,23]; we choose the latter method in the present study for reasons of efficiency.

III. CROSS-SECTION RESULTS FOR Sc^{3+}

We first consider the quantum-mechanical interference between the following recombination pathways:

$$e^- + Sc^{3+}(3p^6)\to Sc^{2+}(3p^5 3d^2)$$

$$\searrow\downarrow$$

$$Sc^{2+}(3p^6 3d)+\omega.$$

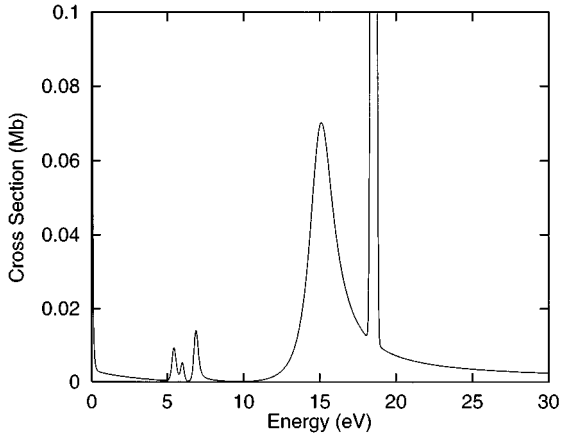

FIG. 1. LS distorted-wave calculation for the Sc^{3+} recombination cross section including the $3p^5 3d^2$ resonances. Solid curve is in the length gauge.

By dipole selection rules only the $3p^6 \epsilon p\ ^2P$ and $3p^6 \epsilon f\ ^2F$ continuum states are allowed to recombine into the $3p^6 3d\ ^2D$ ground state of Sc^{2+}. An LS distorted-wave calculation for the Sc^{3+} recombination cross section, folded with a 0.25 eV Gaussian to simulate the experimental energy resolution, is shown in Fig. 1. A single LS term R-matrix calculation for the Sc^{3+} recombination cross section is shown in Fig. 2. Both methods used bound-state orbitals optimized on the $3p^6 3d$ ground state of Sc^{2+}, obtained from the multiconfiguration Hartree-Fock code of Froese Fischer [25]. The agreement between the two unified calculations in the length gauge is very good. The large resonances at 5.4 eV, 6.9 eV, and 15.0 eV are associated with the three parents of the $3p^5 3d^2\ ^2F$ term in Sc^{2+}, while the three resonances associated with the $3p^5 3d^2\ ^2P$ term are at 6.0 eV, 11.1 eV (which is too narrow and weak to be seen on a convoluted plot of this scale), and 18.6 eV. The large ^2F resonance at 15.0 eV has an extremely large autoionization rate of 2.84×10^{15} sec^{-1} and a quite noticeable asymmetric profile. This is precisely the profile that should be experimentally observable. Additional intermediate coupling (IC) distorted-wave calculations confirm that fine structure splittings have little effect on this broad asymmetric profile.

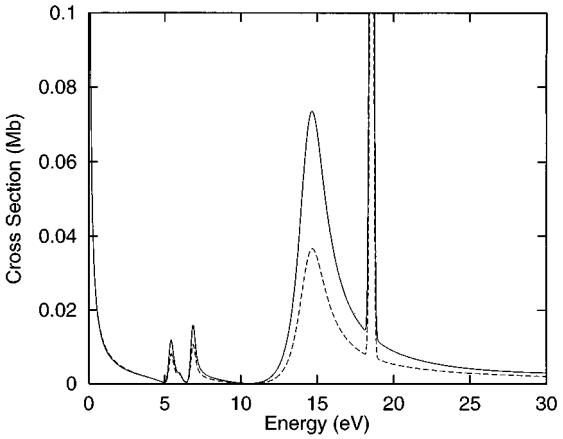

FIG. 2. Single LS term R-matrix calculation for the Sc^{3+} recombination cross section including the $3p^5 3d^2$ resonances. Solid curve is in the length gauge, dashed curve is in the velocity gauge.

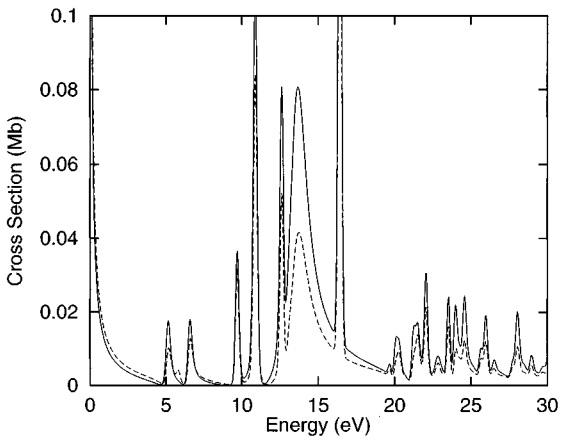

FIG. 3. Seven LS term R-matrix calculation for the Sc^{3+} recombination cross section including the $3p^5 3d^2$ and $3p^5 3dn\ell$ ($n>3$) resonances. Solid curve is in the length gauge, dashed curve is in the velocity gauge.

We next consider the quantum-mechanical interference between the following recombination pathways:

$$e^- + Sc^{3+}(3p^6 + 3p^5 3d) \rightarrow Sc^{2+}(3p^5 3d^2 + 3p^5 3dn\ell)$$

$$\searrow\downarrow$$

$$Sc^{2+}(3p^6 3d + 3p^6 n\ell) + \omega,$$

in an effort to find out whether the stronger and more numerous $3p^5 3dn\ell$ resonances ($n>3$) will wash out the asymmetric $3p^5 3d^2\ ^2F$ resonance profiles. A seven LS term R-matrix calculation for the Sc^{3+} recombination cross section, including the $3p^6$ and $3p^5 3d$ target configurations, is shown in Fig. 3. Although additional resonances appear in the low energy spectrum, the asymmetric profiles of the $3p^5 3d^2\ ^2F$ resonances still survive. Finally, a seven LS term R-matrix calculation for the Sc^{3+} cross section, including $3p^2 \rightarrow 3d^2$ double promotion configurations to take into account the strongest correlation effects in the target and recombined ion, is shown in Fig. 4. In general, all the resonance structures are shifted to slightly higher energies, but

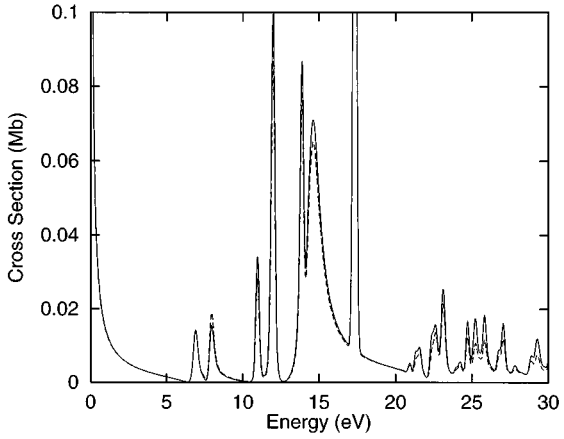

FIG. 4. Correlated seven LS term R-matrix calculation for the Sc^{3+} recombination cross section including the $3p^5 3d^2$ and $3p^5 3dn\ell$ ($n>3$) resonances. Solid curve is in the length gauge, dashed curve is in the velocity gauge.

the strong asymmetric profiles are still present. We note that the length and velocity calculations are now in very good agreement.

The variation of the resonance energies between Figs. 2 and 4 highlights an important aspect of the present calculations, namely, the extreme sensitivity of the resulting resonance profile to the computational details. We find that using orbitals optimized instead on the Sc^{3+} target state yields an energy of the broad $3p^5 3d^2\,^2F$ resonance roughly 1 eV greater than that shown in Fig. 4. Nevertheless, the asymmetric profile of this broad resonance still survives regardless of the computational details.

IV. SUMMARY

In this paper we have carried out unified distorted-wave and close-coupling calculations for the $e^- + Sc^{3+}$ recombination cross section. In the low energy region the calculations predict strong asymmetric resonance profiles due to interference between the radiative and dielectronic recombination pathways. The strength of the asymmetry is quite unusual for electron-ion total recombination cross sections. These distinctive resonance structures should be easily observed in present-day ion storage ring experiments.

ACKNOWLEDGMENTS

M.S.P. was supported in part by the U.S. Department of Energy under Contract No. DE-FG05-96ER54348 with Auburn University, F.R. was supported in part by the NSF under Grant No. NSF-PHY-9457903 with Auburn University, and N.R.B. was supported in part by EPSRC under Contract No. GR/K/14346 with the University of Strathclyde.

[1] P. C. W. Davies and M. J. Seaton, J. Phys. B **2**, 757 (1969).
[2] E. Trefftz, J. Phys. B **3**, 763 (1970).
[3] L. Armstrong, C. E. Theodosiou, and M. J. Wall, Phys. Rev. A **18**, 2538 (1978).
[4] G. Alber, J. Cooper, and A. R. P. Rau, Phys. Rev. A **30**, 2845 (1984).
[5] R. H. Bell and M. J. Seaton, J. Phys. B **18**, 1589 (1985).
[6] V. L. Jacobs, J. Cooper, S. L. Haan, Phys. Rev. A **36**, 1093 (1987).
[7] K. J. LaGattuta, Phys. Rev. A **38**, 1820 (1988).
[8] S. L. Haan and V. L. Jacobs, Phys. Rev. A **40**, 80 (1989).
[9] S. N. Nahar and A. K. Pradhan, Phys. Rev. Lett. **68**, 1488 (1992).
[10] S. N. Nahar and A. K. Pradhan, Phys. Rev. A **49**, 1816 (1994).
[11] F. Robicheaux, T. W. Gorczyca, M. S. Pindzola, and N. R. Badnell, Phys. Rev. A **52**, 1319 (1995).
[12] T. W. Gorczyca, F. Robicheaux, M. S. Pindzola, and N. R. Badnell, Phys. Rev. A **54**, 2107 (1996).
[13] D. A. Knapp, P. Beiersdorfer, M. H. Chen, J. H. Schofield, and D. Schneider, Phys. Rev. Lett. **74**, 54 (1995).
[14] A. Lampert, A. Wolf, D. Habs, J. Kenntner, G. Kilgus, D. Schwalm, M. S. Pindzola, and N. R. Badnell, Phys. Rev. A **53**, 1413 (1996).
[15] M. S. Pindzola, N. R. Badnell, and D. C. Griffin, Phys. Rev. A **46**, 5725 (1992).
[16] M. S. Pindzola, F. Robicheaux, N. R. Badnell, M. H. Chen, and M. Zimmermann, Phys. Rev. A **52**, 420 (1995).
[17] U. Fano Phys. Rev. **124**, 1866 (1961).
[18] H. P. Kelly and R. L. Simons, Phys. Rev. Lett. **30**, 529 (1975).
[19] N. R. Badnell, J. Phys. B **19**, 3827 (1986).
[20] N. R. Badnell, J. Phys. B **30**, 1 (1997).
[21] K. A. Berrington, W. B. Eissner, and P. H. Norrington, Comput. Phys. Commun. **92**, 290 (1995).
[22] N. S. Scott and K. T. Taylor, Comput. Phys. Commun. **25**, 347 (1982).
[23] T. W. Gorczyca, F. Robicheaux, M. S. Pindzola, and N. R. Badnell, Phys. Rev. A **52**, 3852 (1995).
[24] A. P. Hickman, J. Phys. B **17**, L101 (1984).
[25] C. Froese Fischer, Comput. Phys. Commun. **64**, 369 (1991).